J Nanopart Res (2022) 24:64
https://doi.org/10.1007/s11051-022-05447-x

RESEARCH PAPER

Cluster modeling of nanostructurization-driven reamorphization pathways in glassy arsenoselenides: a case study of arsenic monoselenide g-AsSe

O. Shpotyuk · M. Hyla · V. Boyko · Y. Shpotyuk · V. Balitska

Received: 10 January 2022 / Accepted: 27 February 2022

Abstract Nanostructurization-driven reamorphization pathways in glassy arsenic monoselenide g-AsSe originated from both realgar- and pararealgar-type As_4Se_4 molecules are refined employing ab initio quantum-chemical modeling with atomic cluster-simulation code CINCA. At the basis of calculated cluster-forming energies, most possible molecular-to-network disproportionality scenarios are identified in g-AsSe and parameterized in terms of potential energy landscape. The global equilibrium in melt-quenched g-AsSe is shown to be shifted to under-constrained molecular entities of realgar- and pararealgar-type, supplemented by some network-forming derivatives like optimally-constrained single-broken realgar-type clusters. As a result, the glassy network of melt-quenched g-AsSe tends to be more topologically perfect keeping as many as possible small-ring entities. On the contrary, under externally induced nanostructurization activated by nanomilling, the global equilibrium is shifted to over-constrained *reamorphized* network built of chain-like entities without small rings stabilized with nearly the same molecular-to-network disproportionality barrier approaching ~ 0.30 kcal/mol.

Keyword Nanostructurization · Reamorphization · Arsenic monoselenide · Nanomilling

O. Shpotyuk (✉) · M. Hyla
Jan Dlugosz University, 13/15, al. Armii Krajowej, 42200 Czestochowa, Poland
e-mail: olehshpotyuk@yahoo.com

O. Shpotyuk · V. Boyko
Vlokh Institute of Physical Optics, 23, Dragomanov st, Lviv 79005, Ukraine

Y. Shpotyuk
Ivan Franko National University of Lviv, 107, Tarnavskoho st, Lviv 79017, Ukraine

Y. Shpotyuk
Institute of Physics, University of Rzeszow, 1, Pigonia st, 35959 Rzeszow, Poland

V. Balitska
Lviv State University of Life Safety, 35, Kleparivska str, Lviv 79007, Ukraine

Background

Among variety of externally induced inter-phase transitions in solids, amorphous-to-amorphous transitions have attracted a great deal of attention in view of their potential using in contemporary nanomaterials science (Naterer 2003; Ahmad et al. 2016). Many of such transitions can be realized in covalent vitreous chalcogenides like glassy arsenic monoselenide g-AsSe, which is known to possess a few structural conformations associated with molecular- and network-forming entities (Adam and Zhang 2013; Yang et al. 2010; Golovchak et al. 2015; Shpotyuk et al. 2021). It was found that *reversible* amorphous-to-amorphous switching can be initiated optically

Published online: 11 March 2022

in AsSe films prepared by pulsed-laser deposition (Kalyva et al. 2013). Completely renewable breakdown in intermediate range order was also observed in melt-quenched glassy arsenoselenide g-AsSe in compression-decompression cycles (Ahmad et al. 2016). However, from practical implementation point, this polyamorphic transition seems to be more perspective if being realized *irreversibly* as *reamorphization* starting from initial amorphous state I to final amorphous state II stabilized for a relatively long time. Thus, it was found that drastic changes in medium-range ordering of g-AsSe could be caused by modified quenching, when melt was cooled quickly in liquid nitrogen and more slowly in room-temperature water (Dongol and Elhady 2020). Recently, stable network conformations were also observed in bulky g-AsSe subjected to nanostructurization under high-energy mechanical milling (Shpotyuk et al. 2021, 2019, 2020).

The objective of the current research is to refine most plausible *reamorphization* scenarios in glassy arsenic monoselenide g-AsSe employing ab initio quantum-chemical modeling based on cluster-simulation code CINCA (Shpotyuk et al. 2013, 2015; Shpotyuk and Hyla 2017).

The method: ab initio quantum-chemical modeling of molecular- and network-forming structural conformations in g-AsSe by atomic cluster-simulation code CINCA

The optimized configurations of As_4Se_4 molecules in different topological conformations and their network-forming derivatives (iso-compositional with g-AsSe) responsible for reamorphization were refined by ab initio quantum-chemical modeling developed within cation-interlinking network cluster approach, CINCA (Shpotyuk et al. 2013, 2015; Shpotyuk and Hyla 2017). Network-forming clusters were reconstructed by breaking As_4Se_4 molecule on distinct fragments linked with surrounding by homonuclear $Se_{1/2}$…$Se_{1/2}$ bridges. The HyperChem Release program based on restricted Hartree–Fock self-consistent field method with split-valence double-zeta basis set and single polarization function 6-311G* (Hehre et al. 1969; McLean and Chandler 1980) was used to calculate cluster-forming energies E_f. Geometrical optimization and single-point energy calculations were performed with Fletcher-Reeves conjugate gradient method until the root-mean-square gradient of 0.1 kcal/(Å·mol) was reached. The E_f energies were corrected on the energy of terminated H atoms transforming network configuration in self-consistent molecular one in accord to procedure developed elsewhere (Shpotyuk et al. 2013; Jackson 2000; Holomb et al. 2009) and determined in respect to the energy of $AsSe_{3/2}$ pyramid of -72.309 kcal/mol (Shpotyuk et al. 2015).

Results and discussion

The cage-like As_4Se_4 molecule of D_{2d} symmetry composing the structure of monoclinic tetra-arsenic tetra-selenide (Renninger and Averbach 1973), iso-typical with "building" molecular unit of mineral realgar (r) α-As_4S_4 (Ito et al. 1952; Mullen and Nowacki 1972), is main source for amorphization in directly-synthesized g-AsSe alloy subjected to nanostructurization through high-energy mechanical milling (Shpotyuk et al. 2021). In addition, an alternative amorphization pathway from pararealgar-type pr-As_4Se_4 molecule of C_s symmetry iso-typical with principal "building" unit of pararealgar pr-As_4S_4 (which is metastable modification of tetraarsenic tetrasulfide (Bonazzi and Bindi 2008)), is also to be considered in an overall picture of this polyamorphic amorphous-to-amorphous transition.

Reamorphization scenarios derived from realgar-type r-As_4Se_4 molecule

Cluster-forming energies E_f of realgar-type r-As_4Se_4 molecule and network-forming clusters derived from this molecule by breaking in respective Se atom positions (determined in respect to the energy of single trigonal $AsSe_{3/2}$ pyramid) are gathered in Table 1. Some characteristics of these clustering configurations such as number of small-ring entities (hexagons and/or pentagons), and atom-averaged constraints n_c calculated via the Phillips-Thorpe constraint-counting algorithm, assuming stretching/bending forces for intra-cluster bonds (Phillips 1979; Thorpe 1983, 1995) are also included in this Table 1.

The optimized configuration of **realgar-type× 0-r-As_4Se_4 molecule** (without breaks) refined from quantum-chemical modeling using cluster-simulation

Table 1 Cluster-forming energies E_f determined in respect to the energy of trigonal $AsSe_{3/2}$ pyramid for realgar-type r-As_4Se_4 molecule and its network-forming derivatives (the levels of Se atoms refer to Fig. 1a)

Molecular cluster	Network cluster and cluster-forming pathway	Short rings: hexa-penta-gons	n_c	E_f, kcal/mol
×0-r-As_4Se_4	No break (×0-break)	4–4	2.875	0.40
$As_4Se_5H_2$	×1-r-As_4Se_4 – single break in one Se atom position (Se1)	1–2	3.00	0.25
$As_4Se_6H_4$	×2–1-r-As_4Se_4 – double break in two adjusted Se atom positions (Se1, Se3)	0–1	3.125	−0.42
$As_4Se_6H_4$	×2–2-r-As_4Se_4 – double break in two opposite Se atom positions (Se1, Se4)	1–0	3.25	−9.64
$As_4Se_7H_6$	×3-r-As_4Se_4 – triple break in three Se atom positions (Se2, Se3, Se4)	0–0	3.25	0.045
$As_4Se_8H_8$	×4-r-As_4Se_4 – quadruple break in four Se atom positions (Se1, Se2, Se3, Se4)	0–0	3.25	0.11

code CINCA is reproduced on Fig. 1a. This molecule of D_{2d} symmetry is built of four twofold coordinated Se and four threefold coordinated As atoms forming maximum number of small rings, these being four *pentagons* and four *hexagons* built of eight heteronuclear As-Se bonds and two homonuclear As-As bonds in opposite-orthogonal configuration. The calculated cluster-forming energy E_f of this molecule approaches 0.40 kcal/mol, which is the absolutely dominated value among all clusters of this type. If glass network is formed from these ×0-r-As_4Se_4 cages, the number of atom-averaged constraints n_c is 2.875 (that is smaller than space dimensionality), corresponding to under-constrained floppy network. The geometrically optimized parameters of this molecule (in Table 2) are in good agreement with intramolecular bond distances and angles refined from its crystalline counterpart, the monoclinic tetrameric arsenic selenide As_4Se_4 (see, (Renninger and Averbach 1973; Bastow and Whitfield 1973; Smail and Sheldrick 1973; Goldstein and Paton 1974)). Thus, in this cluster, the equivalent directly bonded As-Se distances occur to be close to ~ 2.38 Å, As-As bond distances are compactly grouped around ~ 2.55 Å and inter-bond angles ∠Se-As-Se, ∠As-Se-As, and ∠As-As-Se approach 94.5°, 97.5°, and 101.4°, respectively. The high symmetry of this ×0-r-As_4Se_4 cage-like molecule is confirmed by small deviations in calculated values of the above interatomic bond distances and angles.

Among five network-forming derivatives of ×0-r-As_4Se_4 molecule, the smallest cluster-forming energy E_f = 0.25 kcal/mol is character for cluster produced by **single × 1-breaking**, in one of Se atom positions, which has $As_4Se_5H_2$ molecular prototype shown on Fig. 1b. This cluster (×1-r-As_4Se_4), keeping one hexagon and two pentagons, is *optimally constrained* (n_c = 3.00). Due to low barrier with ground state of parent ×0-r-As_4Se_4 molecule (ΔE_f = 0.15 kcal/mol), transition from molecular to network arrangement in g-AsSe occurs as externally activated uphill tunneling, thus forming a governing source of its nanostructurization-driven *reamorphization* (Shpotyuk et al. 2021).

Two network-forming clusters derived from ×0-r-As_4Se_4 molecule by **double × 2-breaking** in two Se atom positions in opposite or adjusted configuration keep one of small rings (pentagon or hexagon) and thus being over-constrained in view of n_c > 3.00. These cluster are not reproduced on Fig. 1, since E_f energies are too unfavorable in comparison with other alternatives (see Table 1).

Under **triple × 3-breaking** in three of four Se positions in ×0-r-As_4Se_4 molecule, resultant cluster (×3-r-As_4Se_4) attains *chain-like* configuration without any small rings, possessing *over-constrained* topology (n_c = 3.25). Molecular prototype of this cluster ($As_4Se_7H_6$) is reproduced on Fig. 1c. The respective intrinsic angular and linear inter-atomic correlations in this cluster slightly differ from those proper to parent realgar-type molecule (see Fig. 1a, Table 2), resulting in very attractive E_f energy approaching 0.05 kcal/mol. Therefore, the structure of nanostructured g-AsSe can be imagined as completely polymerized network of these clusters acting as "building" chains, provided the relatively small portion of energy is gained to this glassy network under nanostructurization.

Under **quadruple × 4-breaking** in all Se atom positions within ×0-r-As_4Se_4 molecule, the glass network (×4-r-As_4Se_4) becomes intrinsically decomposed on distinct $As_2Se_{4/2}$ bridges based on As-As

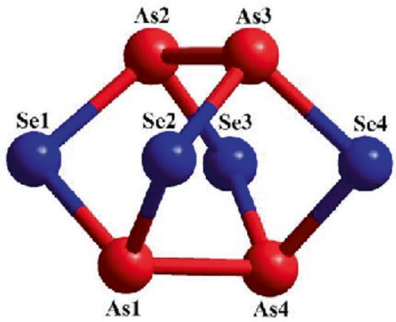

a – realgar-type r-As$_4$Se$_4$ (x0-breaking, no breaks)

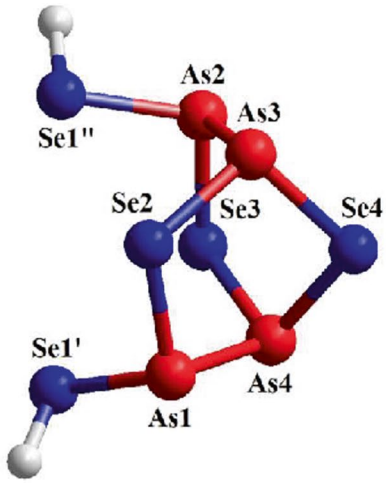

b – As$_4$Se$_5$H$_2$ (x1-breaking)

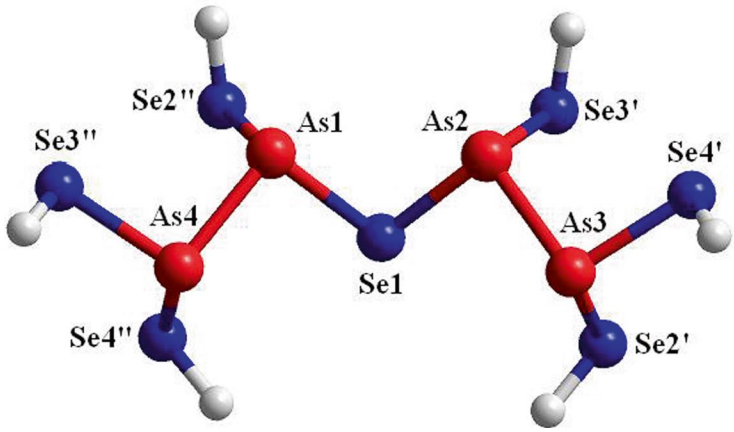

c – As$_4$Se$_7$H$_6$ (x3-breaking)

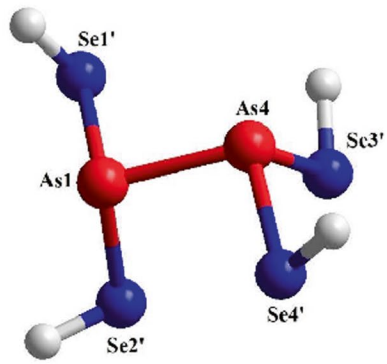

d – As$_4$Se$_7$H$_6$ (x4-breaking)

Fig. 1 Optimized configurations of under-constrained (n_c = 2.875) realgar-type × 0-r-As_4Se_4 cage-like molecule (**a**) and most favorable molecular prototypes of network-forming entities derived from this molecule by single × 1-breaking in one of four Se atom positions (**b**, optimally constrained $As_4Se_5H_2$, n_c = 3.00), triple × 3-breaking in three Se atom positions (**c**, over-constrained $As_4Se_7H_6$, n_c = 3.25), and quadruple × 4-breaking in four Se atom positions (**d**, over-constrained $As_2Se_4H_4$, n_c = 3.25). The terminated H atoms are gray-colored, Se and As atoms are respectively blue- and red-colored, and inter-atomic covalent bonds are depicted by respectively colored sticks

bond previously simulated in Shpotyuk et al. (2015). The optimized configuration of molecular prototype ($As_2Se_4H_4$) of this *over-constrained* cluster (n_c = 3.25) is shown on Fig. 1d. Nevertheless, since difference in the E_f energy with × 3-r-As_4Se_4 cluster (Fig. 1c) is small, this transformation can be considered as complemented to *chain-forming tendency*. In both cases of triple and quadruple breaking in × 0-r-As_4Se_4 molecule, resultant network is chain-like built of distinct $As_2Se_{4/2}$ fragments interlinked by optimally constrained bridges = As-Se-As = (Shpotyuk et al. 2015).

Within different network-forming clusters originated from realgar-type × 0-r-As_4Se_4 molecule, the energetically favorable are those having direct bonded As-As distances d ~ 2.48 Å, while in molecular conformation, these distances are evidently longer close to d ~ 2.55 Å (see Table 2). This is character for optimally constrained (n_c = 3.00) single-broken × 1-r-As_4Se_4 network clusters, and over-constrained (n_c = 3.25) triple-broken × 3-r-As_4Se_4 and quadruple-broken × 4-r-As_4Se_4 chain clusters. In contrast, a huge energy gain (E_f = -9.64 kcal/mol,

Table 2 Geometrically optimized parameters (interatomic distances *d* and bond angles *α*) in realgar-type r-As_4Se_4 molecule (the atom labels refer to Fig. 1a)

Equivalent bond distances				Equivalent bond angles		
Atoms	***d*, Å**	**Atoms**	***d*, Å**	***α***		**(deg.) °**
Direct bonded distances				**∠ Se-As-Se**		
As–As	As2–Se1	2.3765	∠ Se1-As1-Se2	94.538		
As1–As4	2.5515	As2–Se3	2.3766	∠ Se1-As2-Se3	94.515	
As2–As3	2.5520	As3–Se2	2.3764	∠ Se2-As3-Se4	94.527	
As–Se	As3–Se4	2.3762	∠ Se3-As4-Se4	94.537		
As1–Se1	2.3764	As4–Se3	2.3763			
As1–Se2	2.3766	As4–Se4	2.3767	**∠ As-Se-As**		
Non-bonded distances				∠ As1-Se1-As2	97.531	
As–As		**As–Se**		∠ As1-Se2-As3	97.542	
As1–As2	3.5742	As1–Se3	3.8145	∠ As2-Se3-As4	97.532	
As1–As3	3.5747	As1–Se4	3.8155	∠ As3-Se4-As4	97.545	
As2–As4	3.5743	As2–Se2	3.8155	**∠ Se-As-As**		
As3–As4	3.5746	As2–Se4	3.8147	∠ Se1-As1-As4	101.412	
Se–Se		As3–Se3	3.8161	∠ Se2-As1-As4	101.384	
Se1–Se2	3.4913	As3–Se1	3.8153	∠ Se1-As2-As3	101.394	
Se1–Se3	3,4907	As4–Se1	3.8153	∠ Se3-As2-As3	101.419	
Se1–Se4	4.9370	As4–Se2	3.8147	∠ Se2-As3-As2	101.401	
Se2–Se3	4.9370			∠ Se4-As3-As2	101.376	
Se2–Se4	3.4907			∠ Se3-As4-As1	101.384	
Se3–Se4	3.4913			∠ Se4-As4-As1	101.409	

see Table 1) should be transferred in glassy network reconstructed from double-broken × 2–2-r-As_4Se_4 clusters to accommodate asymmetric hexagon with intrinsic homonuclear As-As bond distances unrealistically approaching ~ 2.27 Å and disturbed heteronuclear As-Se bond distances extended to ~ 4.8 Å and shortened to ~ 2.3 Å. Another network configuration built from × 0-r-As_4Se_4 molecule by breaking in two adjusted Se positions is also unfavorable since E_f = -0.42 kcal/mol (see Table 1), needed to allocate a set of highly deviated As-Se bond distances approaching ~ 2.38, ~ 2.40, and ~ 2.45 Å within the same short ring (pentagon).

Reamorphization scenarios derived from pararealgar-type pr-As_4Se_4 molecule

Cluster-forming energies E_f of pararealgar-type × 0-pr-As_4Se_4 molecule and derivatives built from this molecule by breaking in respective Se atom positions, along with topological characteristics of these network-forming clusters (including the number of short-ring entities, hexagons-pentagons-tetragons) are gathered in Table 4.

The optimized configuration of **pararealgar-type × 0-pr-As_4Se_4 molecule** refined from quantum-chemical CINCA modeling is reproduced on Fig. 2a. This molecule of C_s symmetry is composed of eight heteronuclear As-Se bonds and two homonuclear As-As bonds in neighboring configuration forming four small rings, these being one *hexagon*, two *pentagons*, and one *tetragon*. The cluster-forming energy E_f of this molecule approaches 0.30 kcal/mol (respectively to $AsSe_{3/2}$), the quite competitive as compared with realgar-type × 0-r-As_4Se_4 molecule shown on Fig. 1a. The glassy network built of such units is also under-constrained since n_c = 2.75.

The optimized parameters of × 0-pr-As_4Se_4 molecule are gathered in Table 5. Since crystalline counterpart built of this molecule is unknown, we compare them with parameters proper to iso-compositional realgar-type crystalline analogue, the monoclinic tetraarsenic tetraselenide As_4Se_4 (Renninger and Averbach 1973; Bastow and Whitfield 1973; Smail and Sheldrick 1973; Goldstein and Paton 1974). Thus, in respect to our calculations (see Table 5), direct heteronuclear As-Se bond distances in this molecule are averaged around ~ 2.39 Å,

while homonuclear As-As distances are averaged around ~ 2.49 Å. The interbond angles ∠Se-As-Se, ∠As-Se-As, ∠As-As-Se, ∠As-As-As approach 102.8°, 100.9°, 85.6° and 88.2°, respectively. The similar distribution of structural parameters can be traced in realgar α-As_4S_4 (see, (Ito et al. 1952; Mullen and Nowacki 1972; Bonazzi and Bindi 2008)) as compared with its metastable polymorph, the pararealgar pr-As_4S_4 (see, (Bonazzi et al. 1995)). This finding confirms realistic possibility to stabilize pararealgar-type × 0-pr-As_4Se_4 molecules in melt-quenched arsenic monoselenide g-AsSe.

Among network-forming clusters related to pararealgar-type × 0-pr-As_4Se_4 molecule, three ones can be formed by single × 1-breaking or triple × 3-breaking, four ones can be formed by double × 2-breaking, and one cluster can be formed by **quadruple × 4-breaking** in all Se atom positions (see Table 4). However, despite this variety, only the latter (× 4-pr-As_4Se_4) is worth to be considered as quite competitive to the above network-forming clusters. Indeed, this over-constrained cluster (in nview of $n_c = 3.25$) is characterized by low E_f energy approaching − 0.03 kcal/mol, that is close to this energy for optimally constrained trigonal $AsSe_{3/2}$ pyramid (see, (Shpotyuk et al. 2015)). Molecular prototype of this cluster ($As_4Se_8H_8$) is shown on Fig. 2b–2c. In fact, this cluster introduces decomposition in glassy network on two *chain-forming* parts, these being (i) over-constrained one ($n_c = 3.36$) with $As_3Se_5H_5$ molecular prototype forming chain of neighboring atom-shared As-As bonds (see Fig. 2b) and (ii) optimally constrained one ($n_c = 3.00$) with $AsSe_3H_3$ prototype forming chain of atom-shared $AsSe_{3/2}$ pyramids (see Fig. 2c). The calculated geometrically optimized parameters of the former (i) are gathered in Table 6, the parameters of the latter (ii) are given in our previous work (Shpotyuk et al. 2015). Noteworthy, the refined values of direct interatomic bond distances and intrinsic interbond angles in chain-like network-forming structures originated from both realgar-type r-As_4Se_4 (see Table 3) and pararealgar-type pr-As_4Se_4 (see Table 6) molecules occur to be very similar, speaking in favor of the same global tendency towards chain-like conformation in g-AsSe under nanostructurization.

Expected pathways of nanostructurization-driven reamorphization in g-AsSe

Thus, nanostructurization in glassy arsenic monoselenide g-AsSe is determined by transitions from preferentially under-constrained molecular to over-constrained network matrix with obviously dominated chain-like structural conformations (also over-constrained). Diversity of these transitions is illustrated by unified potential energy landscape on Fig. 3 showing most possible molecular-to-network disproportionality pathways in g-AsSe originated from states of realgar- and pararealgar-type As_4Se_4 molecules (× 0-r-As_4Se_4 and × 0-pr-As_4Se_4).

The network of g-AsSe related to realgar-type entities is stabilized under balance between × 0-r-As_4Se_4 cage-like molecules ($E_f = 0.40$ kcal/mol) and some network-forming derivatives, these being (in a sequence of growing molecular-to-network transition barrier, ΔE_f) single-broken × 1-r-As_4Se_4 ($\Delta E_f = 0.15$ kcal/mol), quadruple-broken × 4-r-As_4Se_4 ($\Delta E_f = 0.29$ kcal/mol) and triple-broken × 3-r-As_4Se_4 ($\Delta E_f = 0.35$ kcal/mol), stabilized via the following reactions:

$$x0 - r - As_4Se_4\left(n_c = 2.875\right) \rightarrow x1 - r - As_4Se_4\left(n_c = 3.00\right) + \left(\Delta E_f = 0.15 kcal/mol\right) \quad (1)$$

$$x0 - r - As_4Se_4\left(n_c = 2.845\right) \rightarrow x4 - r - As_4Se_4\left(n_c = 3.25\right) + \left(\Delta E_f = 0.29 kcal/mol\right) \quad (2)$$

$$x0 - r - As_4Se_4\left(n_c = 2.875\right) \rightarrow x3 - r - As_4Se_4\left(n_c = 3.25\right) + \left(\Delta E_f = 0.35 kcal/mol\right) \quad (3)$$

It seems that pararealgar-type entities may contribute to these disordering scenarios through balance between × 0-pr-As_4Se_4 molecules ($E_f = 0.30$ kcal/mol) and quadruple-broken × 4-pr-As_4Se_4 derivatives ($\Delta E_f = -0.03$ kcal/mol), stabilized via molecular-to-network disproportionality reaction:

$$x0 - pr - As_4Se_4\left(n_c = 2.75\right) \rightarrow x4 - pr - As_4Se_4\left(n_c = 3.25\right) + \left(\Delta E_f = 0.33\ kcal/mol\right) \quad (4)$$

Table 3 Geometrically optimized parameters (interatomic distances d and bond angles α) in × 3-broken network chain-like cluster derived from realgar-type r-As_4Se_4 molecule by triple breaking in three Se atom positions (the atom labels refer to Fig. 1c)

Equivalent bond distances				Equivalent bond angles	
Atoms	***d*, Å**	**Atoms**	***d*, Å**	***α***	**(deg.) °**
Direct bonded distances				**∠ Se-As-Se**	
As–As		As2–Se1	2.3966	∠ Se3″-As4-Se4”	99.072
As1–As4	2.4752	As2–Se3’	2.3934	∠ Se2’-As3-Se4’	99.313
As2–As3	2.4760	As3–Se2’	2.3957	∠ Se1-As2-Se3’	100.645
As–Se		As3–Se4’	2.3896	∠ Se1-As1-Se2”	101.281
As1–Se2”	2.3931	As4–Se3”	2.3893		
As1–Se1	2.3978	As4–Se4”	2.3966		
Non-bonded distances				**∠ As-Se-As**	
As–As		**Se – Se**		∠ As1-Se1-As2	96.646
As1–As2	3.5809	Se2’–Se4’	3.6473		
As2–As4	5.4231	Se1–Se3’	3.6866		
As1–As3	5.4233	Se1–Se2”	3.7042		
As3–As4	6.5018	Se2″–Se3”	3.9679		
As–Se		Se2″–Se4”	3.9887	**∠ Se-As-As**	
As1–Se3”	3.5862	Se3″–Se4”	3.9887	∠ Se3″-As4-As1	94.971
As2–Se4’	3.5887	Se3’–Se4’	3.9901	∠ Se4’-As3-As2	95.029
As4–Se1	3.6026	Se2’–Se3’	3.9974	∠ Se1-As1-As4	95.329
As3–Se1	3.6068	Se1–Se2’	4.0741	∠ Se1-As2-As3	95.488
As4–Se2”	3.8131	Se1–Se4”	4.0765	∠ Se2″-As1-As4	103.103
As3–Se3’	3.8222	Se2″–Se3’	5.5139	∠ Se3’-As2-As3	103.415
As1–Se4”	3.8567	Se1–Se3”	5.5312	∠ Se4″-As4-As1	104.663
As2–Se2’	3.8569	Se1–Se4’	5.5343	∠ Se2’-As3-As2	104.674
As1–Se3’	5.0415	Se2’–Se4”	7.3117		
As2–Se2”	5.0525	Se3’–Se4”	7.4869		
As1–Se2’	6.4066	Se2’–Se2”	7.5144		
As2–Se4”	6.4085	Se3’–Se3”	8.5791		
As4–Se3’	7.0917	Se2″–Se4’	8.5959		
As2–Se3”	7.1042	Se2’–Se3”	9.4858		
As1–Se4’	7.1057	Se4’–Se4”	9.4959		
As3–Se2”	7.1101	Se3″–Se4’	10.5031		
As4–Se2’	7.2925				
As3–Se4”	7.3062				
As3–Se3”	8.6011				
As4–Se4’	8.6034				

At the basis of the calculated molecular-to-network barriers, it can be concluded that global equilibrium in melt-quenched g-AsSe is shifted to under-constrained molecular entities of realgar- ($n_c = 2.875$) and pararealgar-type ($n_c = 2.75$), supplemented by admixture of energetically favorable network derivatives like optimally constrained × 1-r-As_4Se_4 clusters ($n_c = 3.00$), formed in respect to reaction (1). So, the network of melt-quenched g-AsSe tends to be more perfect keeping as many as possible small rings (hexagons, pentagons and tetragons, see Tables 1 and 4).

Under more non-equilibrium conditions of externally induced nanostructurization such as those caused by nanomilling producing a huge number of structural defects (see, e.g., (Shpotyuk et al. 2021, 2019, 2020)), the global equilibrium is shifted to over-constrained ($n_c = 3.25$) network derivatives forming preferentially chain structures stabilized via molecular-to-network disproportionality reactions

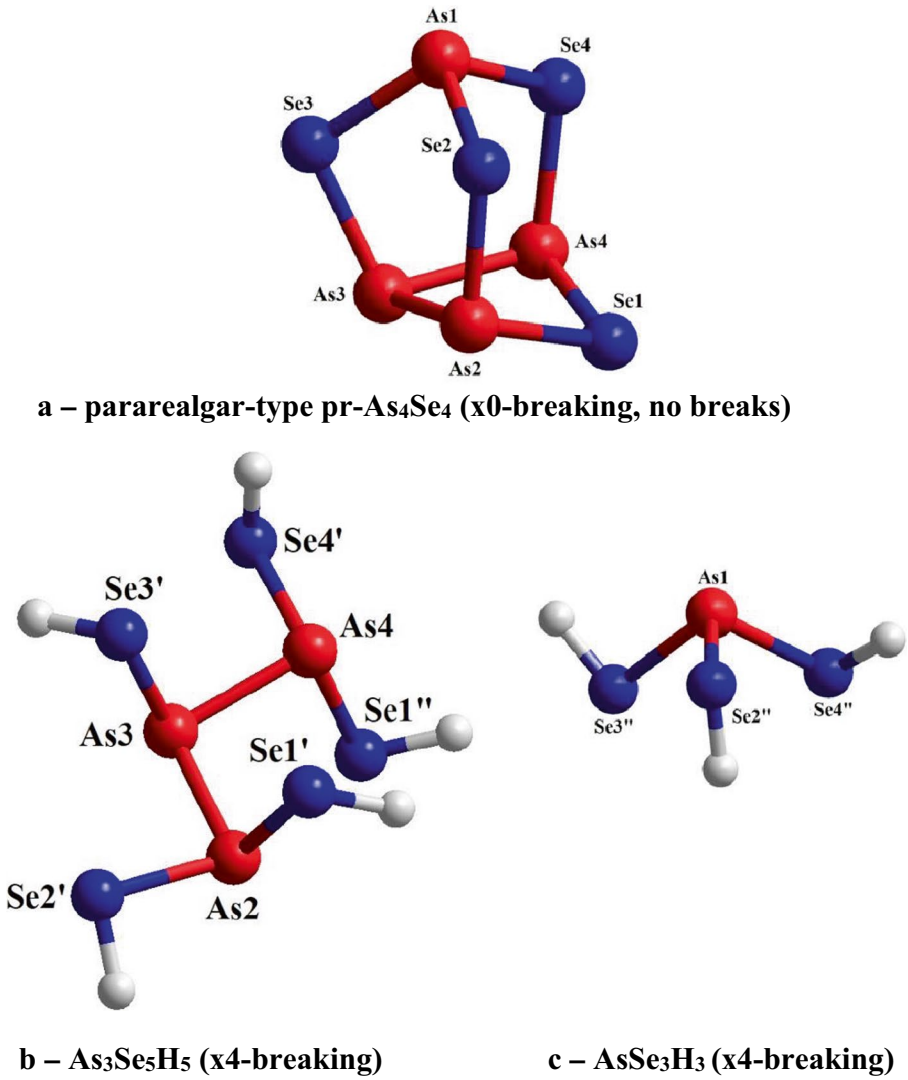

Fig. 2 Optimized configurations of under-constrained ($n_c = 2.75$) pararealgar-type × 0-pr-As_4Se_4 molecule (**a**) and most favorable molecular prototype of over-constrained ($n_c = 3.25$) network-forming cluster derived from this molecule by quadruple × 4-breaking in four Se atom positions $As_4Se_8H_8$ (**b** and **c**) separated on distinct over-constrained ($n_c = 3.36$) $As_3Se_5H_5$ (**b**) and optimally-constrained ($n_c = 3.00$) $AsSe_3H_3$ (c) molecules

(2), (3), and (4) with nearly the same ΔE_f barrier approaching ~ 0.30 kcal/mol. The *reamorphized* matrix of nanostructurized g-AsSe tends to be more defective (topologically stress and rigid) keeping mainly chain-like entities without any small rings (see Fig. 1c and 1d; Fig. 2b and 2c). The global chain-like character of the resultant structural matrix stabilized in reamorphized g-AsSe is confirmed by close similarity between geometrically optimized parameters (directly bonded heteronuclear As-Se and homonuclear As-As bond distances and inter-bond angles) character to × 3-r-As_4Se_4 and × 4-pr-As_4Se_4 network-forming clusters respectively given in Tables 6 and 5.

Conclusions

Competitive nanostructurization scenarios in glassy arsenic monoselenide g-AsSe originated from realgar-type and pararealgar-type As_4Se_4 molecular entities are refined employing ab initio quantum-chemical modeling with atomic cluster-simulation code CINCA. At the basis of calculated cluster-forming energies, the most possible molecular-to-network disproportionality pathways driven by nanostructurization in g-AsSe are identified on potential energy landscape.

The global equilibrium in melt-quenched g-AsSe is shifted towards under-constrained molecular entities of realgar- and pararealgar-type, supplemented by admixture of network derivatives such

Table 4 Cluster-forming energies E_f determined in respect to the energy of trigonal $AsSe_{3/2}$ pyramid for pararealgar-type pr-As_4Se_4 molecule and its network-forming derivatives (the labels of Se atoms refer to Fig. 2a)

Molecular cluster	Network cluster and cluster-forming pathway	Short rings: hexa-penta-tetragons	n_c	E_f, kcal/mol
×0-pr-As_4Se_4	no break (×0-breaking)	1 – 2—1	2.75	0.30
$As_4Se_5H_2$	×1–1-pr-As_4Se_4 – single break in one Se atom position (Se1)	0—2—0	3.00	− 0.25
$As_4Se_5H_2$	×1–2-pr-As_4Se_4 – single break in one Se atom position (Se2)	0—1—1	2.875	− 1.39
$As_4Se_5H_2$	×1–3-pr-As_4Se_4 – single break in one Se atom position (Se3)	1—0—1	3.00	− 1.55
$As_4Se_6H_4$	×2–1-pr-As_4Se_4 – double break in two Se atom positions (Se2, Se4)	0—0—1	3.125	− 4.93
$As_4Se_6H_4$	×2–2-pr-As_4Se_4 – double break in two Se atom positions (Se1, Se2)	0—1—0	3.125	− 7.36
$As_4Se_6H_4$	×2–3-pr-As_4Se_4 – double break in two Se atom positions (Se2, Se3)	0—0—1	3.25	− 9.78
$As_4Se_6H_4$	×2–4-pr-As_4Se_4 – double break in two Se atom positions (Se1, Se3)	1—0—0	3.25	− 5.66
$As_4Se_7H_6$	×3–1-pr-As_4Se_4 – triple break in three Se atom positions (Se2, Se3, Se4)	0—0—1	3.00	− 0.85
$As_4Se_7H_6$	×3–2-pr-As_4Se_4 – triple break in three Se atom positions (Se1, Se2, Se4)	0—0—0	3.25	− 2.81
$As_4Se_7H_6$	×3–3-pr-As_4Se_4 – triple break in three Se atom positions (Se1, Se2, Se3)	0—0—0	3.25	− 0.47
$As_4Se_8H_8$	×4-pr-As_4Se_4 – quadruple break in four Se atom positions (Se1, Se2, Se3, Se4)	0—0—0	3.25	− 0.03

Table 5 Geometrically optimized parameters (interatomic distances d and bond angles α) in pararealgar-type pr-As_4Se_4 molecule (the atom labels refer to Fig. 2a)

Equivalent bond distances				Equivalent bond angles	
Atoms	***d*, Å**	**Atoms**	***d*, Å**	***α***	**(deg.) °**
Direct bonded distances				**∠ Se-As-Se**	
As–As	As1–Se4	2.3829	∠ Se1-As4-Se4	105.263	
As2–As3	2.4874	As3–Se3	2.3486	∠ Se1-As2-Se2	105.272
As3–As4	2.4873	As2–Se1	2.4064	∠ Se2-As1-Se4	105.162
As–Se	As2–Se2	2.3905	∠ Se2-As1-Se3	99.159	
As1–Se2	2.3829	As4–Se1	2.4064	∠ Se3-As1-Se4	99.146
As1–Se3	2.3872	As4–Se4	2.3905	**∠ As-Se-As**	
Non-bonded distances				∠ As2-Se2-As1	105.908
As–As		**As – Se**		∠ As4-Se4-As1	105.928
As1–As2	3.8099	As1–Se1	4.6330	∠ As3-Se3-As1	99.848
As1–As3	3.6239	As2–Se3	3.7933	∠ As2-Se1-As4	92.044
		As2–Se4	4.3382	**∠ Se-As-As**	
		As3–Se1	3.3257	∠ Se3-As3-As2	103.288
Se–Se		As3–Se2	3.8026	∠ Se3-As3-As4	103.304
Se1–Se2	3.8126	As3–Se4	3.8020	∠ Se2-As2-As3	102.421
Se1–Se3	5.0304	As4–Se2	4.3389	∠ Se4-As4-As3	102.400
Se1–Se4	3.8123	As4–Se3	3.7936	∠ Se1-As2-As3	85.604
Se2–Se3	3.6315			∠ Se1-As4-As3	85.606
Se2–Se4	3.7850			**∠ As-As-As**	
Se3–Se4	3.6311			∠ As2-As3-As4	88.245

as optimally constrained single-broken realgar-type clusters. The network of melt-quenched g-AsSe tends to be more topologically perfect keeping as many as possible small rings.

Under non-equilibrium conditions of externally induced nanostructurization such as those caused by nanomilling producing a huge number of defects in g-AsSe, the equilibrium is shifted to over-constrained

Table 6 Geometrically optimized parameters (interatomic bond distances d and bond angles α) in ×4-broken network chain-like cluster derived from pararealgar-type pr-As_4Se_4 molecule by quadruple breaking in four Se atom positions (the atom labels refer to Fig. 2b)

Equivalent bond distances				Equivalent bond angles	
Atoms	***d*, Å**	**Atoms**	***d*, Å**	***α***	**(deg.) °**
Direct bonded distances				**∠ Se-As-Se**	
As–As		**As–Se**		∠ Se1″-As4-Se4’	98.494
As3–As4	2.4747	As2–Se2’	2.3885	∠ Se1’-As2-Se2’	99.390
As2–As3	2.4799	As3–Se3’	2.3962		
As–Se		As4–Se1”	2.3964	**∠ As-As-As**	
As2–Se1’	2.4021	As4–Se4’	2.4023	∠ As2-As3-As4	98.688
Non-bonded distances					
As–As		**Se – Se**		**∠ Se-As-As**	
As2–As4	3.7587	Se1’–Se1”	5.3262	∠ Se1’-As2-As3	105.123
As–Se		Se1’–Se2’	3.6534	∠ Se2’-As2-As3	94.841
As2–Se1”	4.1819	Se1’–Se3’	3.9536	∠ Se3’-As3-As2	102.409
As2–Se3’	3.8007	Se1’–Se4’	6.4091	∠ Se3’-As3-As4	96.071
As2–Se4’	5.7706	Se2’–Se1”	6.3315	∠ Se1″-As4-As3	94.501
As3–Se1’	3.8766	Se2’–Se3’	4.0010	∠ Se4’-As4-As3	97.730
As3–Se1”	3.5774	Se2’–Se4’	7.2392		
As3–Se2’	3.5853	Se3’–Se1”	5.5903		
As3–Se4’	3.6735	Se3’–Se4’	4.4201		
As4–Se1’	4.1875	Se4’–Se1”	3.6351		
As4–Se2’	5.6473				
As4–Se3’	3.6222				

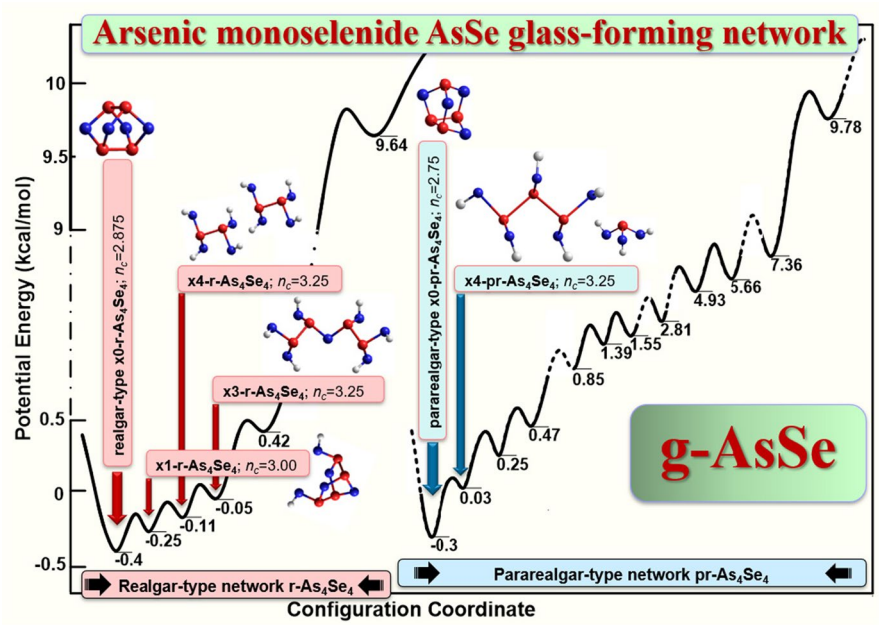

Fig. 3 Unified potential energy landscape of glassy arsenic monoselenide g-AsSe showing diversity in *reamorphization* pathways originated from realgar-type (at the left, red-colored) and pararealgar-type (at the right, blue-colored) As_4Se_4 molecules. The forming energies E_f of molecular As_4Se_4 clusters and their most favorable network derivatives are given below respective potential energy wells highlighted by arrows (the calculated atom-averaged number of constraints n_c is denoted)

reamorphized network built of chain-like structural entities without small rings stabilized with nearly the same molecular-to-network disproportionality barrier of ~ 0.30 kcal/mol.

Funding The paper is part of scientific research done within the project No 0119U100357, subject of Scientific Program funded by Ministry of Education and Science of Ukraine for years 2019–2021.

Declarations

Conflict of interests The authors declare that they have no conflict of interest.

References

Naterer GF (2003) Heat transfer in single and multiphase systems. CRC Press LLC, Boca Raton-London-New York-Washington

Ahmad AS, Glazyrin K, Liermann HP et al (2016) Breakdown of intermediate range order in AsSe chalcogenide glass. J Appl Phys 120:145901-1–145906. https://doi.org/10.1063/1.4964798

Adam J-L, Zhang X (2013) Chalcogenide Glasses: Preparation, properties and application. Woodhead Publ. Ser. in Electronic and Optical Mater, Philadelphia-New Delhi

Yang G, Bureau B, Rouxel T, P, et al (2010) Correlation between structure and physical properties of chalcogenide glasses in the As_xSe_{1-x} system. Phys Rev B 82:195206-1–195208. https://doi.org/10.1103/PhysRevB.82.195206

Golovchak R, Lucas P, Oelgoetz J, Kovalskiy A, York-Winegar J, Saiyasombat C, Shpotyuk O, Feygenson M, Neuefeind J, Jain H (2015) Medium range order and structural relaxation in As–Se network glasses through FSDP analysis. Mater Chem Phys 153:432–442. https://doi.org/10.1016/j.matchemphys.2015.01.037

Shpotyuk Y, Demchenko P, Shpotyuk O, Balitska V, Boussard-Pledel C, Bureau B, Lukáčová Bujňáková Z, Baláž P (2021) High-energy mechanical milling-driven *reamorphization* in glassy arsenic monoselenide g-AsSe: on the path tailoring special molecular-network glasses. Materials 14:4478–1–14. https://doi.org/10.3390/ma14164478

Kalyva M, Orava J, Siokou A, Pavlista M, Wagner T, Yannopoulos SN (2013) Reversible amorphous-to-amorphous transitions in chalcogenide films: correlating changes in structure and optical properties. Adv Funct Mater 23:2052–2059. https://doi.org/10.1002/adfm.201202461

Dongol M, Elhady AF (2020) Preparation conditions and medium range order modification of As-Se glasses. Phys B583:412027-1–412034. https://doi.org/10.1016/j.physb.2020.412027

Shpotyuk Y, Boussard-Pledel C, Bureau B, Demchenko P, Szlęzak J, Cebulski J, Bujňáková Z, Baláž P, Shpotyuk O (2019) Effect of high-energy mechanical milling on the FSDP-related XRPD correlations in Se-rich glassy arsenic selenides. J Phys Chem Sol 124:318–326. https://doi.org/10.1016/j.jpcs.2018.09.036

Shpotyuk Y, Demchenko P, Bujňáková Z, Baláž P, Boussard-Pledel C, Bureau B, Shpotyuk O (2020) Effect of high-energy mechanical milling on the medium-range ordering in glassy As-Se. J Am Ceram Soc 103:1631–1646. https://doi.org/10.1111/jace.16877

Shpotyuk O, Hyla M, Boyko V (2013) Structural-topological genesis of network-forming nanoclusters in chalcogenide semiconductor glasses. J Optoelectron Adv Mater 15:1429–1437

Shpotyuk O, Hyla M, Boyko V (2015) Compositionally-dependent structural variations in glassy chalcogenides: The case of binary As-Se system. Comput Mater Sci 110:144–151. https://doi.org/10.1016/j.commatsci.2015.08.015

Shpotyuk O, Hyla M (2017) Compositionally-dependent network-forming tendencies in S-rich As-S glasses. J Optoelectron Adv Mater 19:48–56

Hehre WJ, Stewart RF, Pople JA (1969) Self-consistent molecular-orbital methods. I. Use of Gaussian expansions of slater-type atomic orbitals. J Chem Phys 51:2657–2665. https://doi.org/10.1063/1.1672392

McLean AD, Chandler GS (1980) Contracted Gaussian basis sets for molecular calculations. I. Second row atoms, Z=11-18. J Chem Phys 72:5639–5648. https://doi.org/10.1063/1.438980

Jackson K (2000) Electric fields in electronic structure calculations: electric polarizabilities and IR and Raman spectra from first principles. Phys Stat Solidi B217:293–310. https://doi.org/10.1002/3527603107.ch12

Holomb R, Veres M, Mitsa V (2009) Ring-, branchy-, and cage-like As_nS_m nanoclusters in the structure of amorphous semiconductors: ab initio and Raman study. J Optoelectron Adv Mater 11:917–923

Renninger A, Averbach B (1973) Crystalline structures of As_2Se_3 and As_4Se_4. Acta Cryst B29:1583–1589. https://doi.org/10.1107/S0567740873005091

Ito T, Morimoto N, Sadanaga R (1952) The crystal structure of realgar. Acta Cryst 5:775–782. https://doi.org/10.1107/S0365110X52002112

Mullen DJE, Nowacki W (1972) Refinement of the crystal structures of realgar, AsS and orpiment, As_2S_3. Z Kristallogr 136:48–65. https://doi.org/10.1524/zkri.1972.136.1-2.48

Bonazzi P, Bindi L (2008) A crystallographic review of arsenic sulfides: effects of chemical variations and changes induced by exposure to light. Z Kristallogr 223:132–147. https://doi.org/10.1524/zkri.2008.0011

Phillips JC (1979) Topology of covalent non-crystalline solids. I: Short-range order in chalcogenide alloys. J Non-Cryst Solids 34:153–181. https://doi.org/10.1016/0022-3093(79)90033-4

Thorpe MF (1983) Continuous deformations in random networks. J Non-Cryst Solids 57:355–370. https://doi.org/10.1016/0022-3093(83)90424-6

Thorpe MF (1995) Bulk and surface floppy modes. J Non-Cryst Solids 182:135–142. https://doi.org/10.1016/0022-3093(94)00545-1

Bastow TJ, Whitfield HJJ (1973) Crystal structure of tetra-arsenic tetraselenide. Chem Soc Dalton Trans 1973:1739–1740. https://doi.org/10.1039/DT9730001739

Smail EJ, Sheldrick GM (1973) Tetra-Arsenic Tetraselenide Acta Cryst B29:2014–2016. https://doi.org/10.1107/S0567740873005972

Goldstein P, Paton A (1974) The crystal and molecular structure of tetrameric arsenic selenide, As_4Se_4. Acta Cryst B30:915–920. https://doi.org/10.1107/S0567740874004043

Bonazzi P, Menchetii S, Pratesi G (1995) The crystal structure of pararealgar, As_4S_4. Am Mineral 80:400–403. https://doi.org/10.2138/am-1995-3-422